Eur. Phys. J. C 13, 255–265 (2000)
Digital Object Identifier (DOI) 10.1007/s100520000321

THE EUROPEAN PHYSICAL JOURNAL C

Measurements of the np total cross section difference $\Delta\sigma_L$ at 1.59, 1.79 and 2.20 GeV

V.I.Sharov[1], S.A.Zaporozhets[1], B.P.Adiasevich[2], N.G.Anischenko[1], V.G.Antonenko[2], L.S.Azhgirey[3], V.D.Bartenev[1], N.A.Bazhanov[4], N.A.Blinov[1], N.S.Borisov[3], S.B.Borzakov[5], Yu.T.Borzunov[1], L.V.Budkin[3,†], V.F.Burinov[3], Yu.P.Bushuev[1], L.P.Chernenko[5], E.V.Chernykh[1], S.A. Dolgii[1], V.M.Drobin[1], G.Durand[6], A.P.Dzyubak[7], A.N.Fedorov[8], V.V.Fimushkin[1], M.Finger[3,9], M.Finger,Jr.[3], L.B.Golovanov[1], G.M.Gurevich[10], A.Janata[3,11], A.V.Karpunin[1,†], B.A.Khachaturov[3], A.D.Kirillov[1], A.D.Kovalenko[1], A.I.Kovalev[4], V.G.Kolomiets[3], A.A.Kochetkov[12], E.S.Kuzmin[3], V.P.Ladygin[1], A.B.Lazarev[3], F.Lehar[6], A. de Lesquen[6], A.A.Lukhanin[7], P.K.Maniakov[1], V.N.Matafonov[3], A.B.Neganov[3], M.S.Nikitina[12], G.P.Nikolaevsky[1], A.A.Nomofilov[1], Tz.Panteleev[5,13], Yu.K.Pilipenko[1], I.L.Pisarev[3], N.M.Piskunov[1], Yu.A.Plis[3], Yu.P.Polunin[2], A.N.Prokofiev[4], P.A.Rukoyatkin[1], O.N.Shchevelev[3], V.A.Shchedrov[4], S.N.Shilov[3], Yu.A.Shishov[1], V.B.Shutov[1], M.Slunečka[3,9], V.Slunečková[3], A.Yu.Starikov[1], G.D.Stoletov[3], L.N.Strunov[1], A.L.Svetov[1], A.P.Tsvinev[1], Yu.A.Usov[3], V.I.Volkov[1], V.P.Yershov[1], A.A.Zhdanov[4], V.N.Zhmyrov[3]

[1] Laboratory of High Energies, JINR, 141980 Dubna, Moscow region, Russia
[2] Russian Scientific Center "Kurchatov Institute", Kurchatova Street 46, 123182 Moscow, Russia
[3] Laboratory of Nuclear Problems, JINR, 141980 Dubna, Moscow region, Russia
[4] Petersburg Nuclear Physics Institute, High Energy Physics Division, 188350 Gatchina, Russia
[5] Frank Laboratory of Neutron Physics, JINR, 141980 Dubna, Moscow region, Russia
[6] DAPNIA, CEA/Saclay, 91191 Gif-sur-Yvette Cedex, France
[7] Kharkov Institute of Physics and Technology, Akademicheskaya Street 1, 310108 Kharkov, Ukraine
[8] Laboratory of Particle Physics, JINR, 141980 Dubna, Moscow region, Russia
[9] Charles University, Faculty of Mathematics and Physics, V Holešovičkách 2, 18000 Praha 8, Czech Republic
[10] Russian Academy of Sciences, Institute for Nuclear Research, 60th Oct. Aniversary Prospect 7A, 117312 Moscow, Russia
[11] Academy of Sciences of the Czech Republic, Nuclear Research Institute, 25068 Řež, Czech Republic
[12] Moscow State University, Faculty of Physics, 119899 Moscow, Russia
[13] Bulgarian Academy of Sciences, Institute for Nuclear Research and Nuclear Energy, Tsarigradsko shaussee boulevard 72, 1784 Sofia, Bulgaria

Received: 19 August 1999 / Published online: 3 February 2000 – © Springer-Verlag 2000

This paper is dedicated to the memory of Rostislav Mikhailovich Ryndin, one of the principal founders of relations for the nucleon-nucleon spin-dependent total cross sections.

Abstract. New results of the neutron-proton spin-dependent total cross section difference $\Delta\sigma_L(np)$ at the neutron beam kinetic energies 1.59, 1.79 and 2.20 GeV are presented. Measurements were performed at the Synchrophasotron of the Laboratory of High Energies of the Joint Institute for Nuclear Research in Dubna. A quasi-monochromatic neutron beam was produced by break-up of extracted polarized deuterons. Neutrons were transmitted through a large polarized proton target. Measurements were performed either with a parallel or an antiparallel beam and target polarizations, both oriented along the beam momentum. The results at the two higher energies were measured with two opposite beam and target polarization directions. Only one target polarization direction was available at 1.59 GeV. The present measurements agree well with existing data. A fast decrease of the $-\Delta\sigma_L(np)$ values with increasing energy above 1.1 GeV was confirmed. The new results are also compared with model predictions and with phase shift analysis fits. The $\Delta\sigma_L$ quantities for isosinglet state I=0, deduced from the measured $\Delta\sigma_L(np)$ values and known $\Delta\sigma_L(pp)$ data, are given.

† Deseased

1 Introduction

In this paper are presented the new results of the spin-dependent neutron-proton total cross section difference $\Delta\sigma_L(np)$, measured in 1997 with a quasi-monochromatic polarized neutron beam and a polarized proton target (PPT). Results were obtained at the central values of 1.59, 1.79 and 2.20 GeV neutron beam kinetic energies.

The free polarized neutron beam was produced by break-up of polarized deuterons accelerated by the Synchrophasotron of the Laboratory of High Energies (LHE) of the Joint Institute for Nuclear Research (JINR) in Dubna. This accelerator provides the highest energy polarized neutron beam, which can be reached now (3.7 GeV).

The measurements were carried out within the nucleon-nucleon experimental program which started in 1995 [1,2]. The aim of the program is to extend studies of np interactions above 1.1 GeV.

For purposes of $\Delta\sigma_L(np)$ measurements, a large Argonne-Saclay polarized proton target (PPT) was reconstructed at Dubna [3,4] and a new polarized neutron beam line [5,6] was used. A set of dedicated neutron detectors with corresponding electronics and data acquisition system [7] were performed. At the beginning of 1995, the first three $\Delta\sigma_L(np)$ data points were successfully measured at the central energies 1.19, 2.49, and 3.65 GeV [1,2]. For purposes of the measurements in 1997, a new PPT polarizing solenoid [8] was developed in LHE.

The nucleon-nucleon (NN) total cross section differences $\Delta\sigma_L$ and $\Delta\sigma_T$ together with the spin-average total cross section σ_{0tot} are measured in pure inclusive transmission experiments. They are linearly related with three non-vanishing imaginary parts of the NN forward scattering amplitudes via optical theorems. They check predictions of available dynamic models and provide an important contribution to databases of phase-shift analyses (PSA). From the measured data it is possible to deduce the $\Delta\sigma_L$ nucleon-nucleon isosinglet ($I = 0$) parts using the existing pp (isotriplet $I = 1$) results.

The total cross section differences for pp scattering were first measured at the ANL-ZGS (USA) and then at TRIUMF (Canada), PSI (Switzerland), LAMPF (USA) and SATURNE II (France). Results cover the energy range from 0.2 to 12 GeV. Other data were measured at 200 GeV at FERMILAB (USA) for pp and $\bar{p}p$ interactions [9]. Measurements with incident charged particles need a different experimental set-up than neutron-proton experiments due to the contribution of electromagnetic interactions. Existing results are discussed in review [10] and in references therein.

For the first time $\Delta\sigma_L(pn)$ results from 0.51 to 5.1 GeV were deduced in 1981 from the $\Delta\sigma_L(pd)$ and $\Delta\sigma_L(pp)$ measurement at the ANL-ZGS [11]. Taking a simple difference between pd and pp results, corrected only for Coulomb-nuclear rescattering and deuteron break-up, yields data in qualitative agreement with the free np results. Correction for Glauber-type rescattering including 3-body state final interactions [12] provides a disagreement [10]. For these reasons, the ANL-ZGS pn results were omitted in many existing PSA databases.

Using free polarized neutrons at SATURNE II, $\Delta\sigma_T$ and $\Delta\sigma_L$ results were obtained at 11 and 10 energies, respectively in the energy range 0.31 and 1.10 GeV [13,14,15]. The Saclay results were soon followed by PSI measurements [16] at 7 energy bins from 0.180 to 0.537 GeV, using a continuous neutron energy spectrum. The PSI and Saclay sets allowed to deduce imaginary parts of np and $I = 0$ spin-dependent forward scattering amplitudes [10,15].

$\Delta\sigma_L(np)$ has also been measured at five energies between 0.484 and 0.788 GeV at LAMPF [17]. A quasi-monoenergetic polarized neutron beam was produced in $pd \Rightarrow n + X$ scattering of longitudinally polarized protons. Large neutron counter hodoscopes have to be used because of the small neutron beam intensity.

To be complete, at low energies, $\Delta\sigma_L(np)$ at 66 MeV was measured at the PSI injector [18], and at 16.2 MeV in Prague (Czech Republic) [19]. $\Delta\sigma_T(np)$ was determined in TUNL (USA) at 9 energies between 3.65 and 11.6 MeV [20], and at 16.2 MeV in Prague [21]. Recently, in TUNL $\Delta\sigma_L(np)$ was measured at 6 energies between 4.98 and 19.7 MeV [22] and $\Delta\sigma_T(np)$ at 3 other energies between 10.7 and 17.1 MeV [23]. The results [22,23] are still unpublished, but appear in the George Washington University and Virginia Polytechnic Institute (GW/VPI) PSA database [24] (SAID SP99).

Only $\Delta\sigma_L(np)$ results were obtained at the JINR accelerator at high energy. All these results smoothly connect with the existing data at lower energies. The $-\Delta\sigma_L(np)$ energy dependence show a fast decrease to zero between 1.1 and 2.0 GeV. The data are compared with model predictions and with the PSA fits. Values of the $I = 0$ part of $\Delta\sigma_L$ are also presented.

In Sect. 2 we give a brief determination of observables. In Sect. 3 is described the method of the measurement and an incomplete target filling is treated. The essential details concerning the beam, the polarimeters, the experimental set-up and PPT are given in Sect. 4. The data acquisition and analyses are described in Sect. 5. The results and discussion are presented in Sect. 6.

2 Determination of observables

Throughout this paper we use the NN formalism and the notations for the elastic nucleon-nucleon scattering observables from [25].

The general expression of the total cross section for a polarized nucleon beam transmitted through a PPT, with arbitrary directions of beam and target polarizations, $\vec{P}_B$ and $\vec{P}_T$, respectively, was first deduced in [26,27]. Taking into account fundamental conservation laws, it is written in the form :

$$\sigma_{tot} = \sigma_{0tot} + \sigma_{1tot}(\vec{P}_B, \vec{P}_T) + \sigma_{2tot}(\vec{P}_B, \vec{k})(\vec{P}_T, \vec{k}), \quad (2.1)$$

where $\vec{k}$ is a unit vector in the direction of the beam momentum. The term σ_{0tot} is the total cross section for unpolarized particles, σ_{1tot}, σ_{2tot} are the spin-dependent contributions. They are related to the measurable observables

$\Delta\sigma_T$ and $\Delta\sigma_L$ by :

$$-\Delta\sigma_T = 2\sigma_{1tot}, \tag{2.2}$$

$$-\Delta\sigma_L = 2(\sigma_{1tot} + \sigma_{2tot}), \tag{2.3}$$

called "total cross section differences". The negative signs for $\Delta\sigma_T$ and $\Delta\sigma_L$ in (2.2) and (2.3) correspond to the usual, although unjustified, convention in the literature. The total cross section differences are measured with either parallel or antiparallel beam and target polarization directions. Polarization vectors are transversally oriented with respect to $\vec{k}$ for $\Delta\sigma_T$ measurements and longitudinaly oriented for $\Delta\sigma_L$ experiments. Only $\Delta\sigma_L$ measurements are treated below, but the formulae are similar for both total cross section differences.

For $\vec{P}_B^{\pm}$ and $\vec{P}_T^{\pm}$, all oriented along $\vec{k}$, we obtain four total cross sections :

$$\sigma(\rightrightarrows) = \sigma(++) = \sigma_{0tot} + |P_B^+ P_T^+|\ (\sigma_{1tot} + \sigma_{2tot}), \tag{2.4a}$$

$$\sigma(\leftrightarrows) = \sigma(-+) = \sigma_{0tot} - |P_B^- P_T^+|\ (\sigma_{1tot} + \sigma_{2tot}), \tag{2.4b}$$

$$\sigma(\rightleftarrows) = \sigma(+-) = \sigma_{0tot} - |P_B^+ P_T^-|\ (\sigma_{1tot} + \sigma_{2tot}), \tag{2.4c}$$

$$\sigma(\leftleftarrows) = \sigma(--) = \sigma_{0tot} + |P_B^- P_T^-|\ (\sigma_{1tot} + \sigma_{2tot}). \tag{2.4d}$$

The signs in brackets correspond to the $\vec{P}_B$ and $\vec{P}_T$ directions with respect to $\vec{k}$, in this order. In principle, an arbitrary pair of one parallel and one antiparallel beam and target polarization directions determines $\Delta\sigma_L$. By using two independent pairs, we also remove an instrumental asymmetry.

In the following, we will consider the neutron beam and the proton target. Since the $\vec{P}_B$ direction at the Synchrophasotron could be reversed every cycle of the accelerator, it is preferable to calculate $\Delta\sigma_L$ from pairs of ($\rightrightarrows$ and ($\leftrightarrows$), or ($\rightleftarrows$) and ($\leftleftarrows$) measurements with the same $\vec{P}_T$ orientation to avoid long-time efficiency fluctuations of the neutron detectors. Values of $|P_T^+|$ and $|P_T^-|$ are considered to be well known as functions of time. The spin-independent term drops out when taking the difference, and one obtains :

$$\begin{aligned} -\Delta\sigma_L(P_T^+) &= 2\ (\sigma_{1tot} + \sigma_{2tot})^+ \\ &= \frac{2\ [\sigma(\rightrightarrows) - \sigma(\leftrightarrows)]}{(|P_B^+| + |P_B^-|)\ |P_T^+|}, \end{aligned} \tag{2.5a}$$

$$\begin{aligned} -\Delta\sigma_L(P_T^-) &= 2(\sigma_{1tot} + \sigma_{2tot})^- \\ &= \frac{2\ [\sigma(\leftleftarrows) - \sigma(\rightleftarrows)]}{(|P_B^+| + |P_B^-|)\ |P_T^-|}, \end{aligned} \tag{2.5b}$$

The asymmetry, proportional to the mean value of

$$|P_B| = \frac{1}{2}(|P_B^+| + |P_B^-|), \tag{2.6}$$

is continuously monitored by a beam polarimeter.

The instrumental asymmetry cancels out, giving the final results as a simple average

$$\Delta\sigma_L = \frac{1}{2}[\Delta\sigma_L(P_T^+) + \Delta\sigma_L(P_T^-)]. \tag{2.7}$$

This is discussed in detail in Sect. 4.

σ_{0tot}, $\Delta\sigma_T$ and $\Delta\sigma_L$ are linearly related to the imaginary parts of the three independent forward scattering invariant amplitudes $a + b$, c and d via optical theorems:

$$\sigma_{0tot} = (2\pi/K)\ \Im m\ [a(0) + b(0)], \tag{2.8}$$

$$-\Delta\sigma_T = (4\pi/K)\ \Im m\ [c(0) + d(0)], \tag{2.9}$$

$$-\Delta\sigma_L = (4\pi/K)\ \Im m\ [c(0) - d(0)], \tag{2.10}$$

where K is the CM momentum of the incident nucleon. The relations (2.9) and (2.10) allow to extract the imaginary parts of the spin-dependent invariant amplitudes $c(0)$ and $d(0)$ at the angle $\theta = 0°$ from the measured values $\Delta\sigma_L$ and $\Delta\sigma_T$. Note that the optical theorems provide the absolute amplitudes. Using a direct reconstruction of the scattering matrix (DRSA) these absolute amplitudes are determined at $\theta = 0°$ only, whereas at any other angle one common phase remains undetermined. The absolute amplitudes are also determined by PSA at any scattering angle. The PSA and DRSA approaches are complementary phenomenological analyses, as discussed in [28,29].

Using the measured $\Delta\sigma(np)$ values and the existing $\Delta\sigma(pp)$ data at the same energy, one can deduce $\Delta\sigma_{L,T}(I = 0)$ as :

$$\Delta\sigma_{L,T}(I = 0) = 2\Delta\sigma_{L,T}(np) - \Delta\sigma_{L,T}(pp). \tag{2.11}$$

3 Method of measurement

In the transmission experiment we measure which part of incident beam particles remains in the beam after transmission. For the experiments with incident neutrons such a measurement is always relative. The neutron beam has a circular profile, given by preceeding beam collimators. Out of the collimator dimension the neutron flux is zero, within the collimator size the flux is uniform. The neutron beam intensity is monitored by neutron beam monitors, placed upstream from the target. The target material consists of small beads placed in a cylindrical container of the circular profile. The container cover the beam spot and its horizontal axis coincide with the beam axis. The transmission detectors, downstream from the target, are larger than the beam dimensions. Any unscattered beam particle is detected with the same probability.

If N_{in} is the number of neutrons entering the target and N_{out} the number of neutrons transmitted in a counter array of solid angle Ω, then the total cross section $\sigma(\Omega)$ is related to measured quantities :

$$\frac{N_{out}}{N_{in}} = \exp\big(-\sigma(\Omega) \times n \times d\big) = \exp(-F), \tag{3.1}$$

where n is the number of all target atoms per cm^3 d is the target length and N_{out}/N_{in} is the simple transmission ratio. The number of counts of the beam monitor M and of the transmission counter T depend on the efficiency of each detector, i.e. $M = N_{in} \times \eta(M)$ and $T = N_{out} \times \eta(T)$. The extrapolation of $\sigma(\Omega)$ towards $\Omega = 0$ gives the unpolarized total cross section σ_{0tot}.

In the case of an incompletely filled target, the beads inside the container may be differently distributed. Two hypothetical configurations of the beads represent limits to be considered. The first limit occurs, if a lower part of the container cylinder is full over the entire length of the target d and the upper part is empty. Let us call this filling mode "horizontal" (H). The second limit occurs, if the same amount of the material in the container is condensed within a smaller length and cover the beam spot. This kind of filling will be called "vertical" (V). The transmission effect of any other possible bead configuration will be in between the effects of these two filling modes, since an arbitrary bead distribution could be approximated by a flight of stairs. Decreasing the steps of stairs, we obtain any possible shape of the bead volume.

Introducing a filling factor a ($0 \leq a \leq 1$) the transmission ratio for the horizontal and vertical filling modes can be written as

$$NH_{out}/N_{in} = \big(a\ \exp(-F)\big) + (1-a) \qquad (3.2a)$$
$$NV_{out}/N_{in} = \exp(-F\ a)\ . \qquad (3.2b)$$

In the $\Delta\sigma_L(\Omega)$ measurements with a full target, only the number of polarizable hydrogen atoms n_H is important. $\sigma_{tot}(\Omega)$ depends on the polarizations $P_B^{\pm}$ and $P_T^{\pm}$ as shown in (2.4). For $\Omega \to 0$, we obtain $\Delta\sigma_L(\Omega) \to \Delta\sigma_L$. If one sums over the events taken with one fixed target polarizations P_T^+ or P_T^- and using (2.5a) or (2.5b), the double transmission ratios of the measurements with the averaged P_B from (2.6) for the two $\vec{P}_T$ directions become :

$$\frac{N_{out}(++)/N_{in}(++)}{N_{out}(-+)/N_{in}(-+)} = \exp\ (-\Delta\sigma_L(\Omega)\ |P_B\ P_T^+|\ n_H\ d) \qquad (3.3a)$$
$$\frac{N_{out}(--)/N_{in}(--)}{N_{out}(+-)/N_{in}(+-)} = \exp\ (-\Delta\sigma(\Omega)\ |P_B\ P_T^-|\ n_H\ d)\ . \qquad (3.3b)$$

Note that we follow the notation of (2.3).

Thus the neutron detector efficiencies drop out. In the following we put $N = N_{out}/N_{in}$ depending of $\vec{P}_B$ and $\vec{P}_T$ combination and (3.3) provide :

$$-\Delta\sigma_L(\Omega, P_T^+) = \frac{1}{|P_B\ P_T^+|\ n_H\ d} \times \ln\ \left(\frac{N(++)}{N(-+)}\right), \qquad (3.4a)$$
$$-\Delta\sigma_L(\Omega, P_T^-) = \frac{1}{|P_B\ P_T^-|\ n_H\ d} \times \ln\ \left(\frac{N(--)}{N(+-)}\right). \qquad (3.4b)$$

We may neglect the extrapolation of $\Delta\sigma_L(\Omega)$ towards $\Omega = 0$ due to the small sizes of detectors [1,2]. The Saclay-Geneva (SG) PSA [29] at 1.1 GeV shows that for the angles covered by our detectors the resulting $-\Delta\sigma_L$ value decreases by 0.04 mb at this energy. The SG-PSA solution at 1.0 GeV suggests that this possible error decreases with increasing energy.

The ratio of n_H to other target nuclei depends on the target material. The presence of carbon in the PPT beads add the term $\sigma_{tot}(C)$ in (2.4). This term is spin-independent and its contribution drops out in differences (2.5). The same occurs for ^{16}O and ^4He in the target and for the cryogenic envelopes. The np total cross section for all unpolarized atoms is large with respect to the total cross section difference. Above ~ 0.3 GeV neutron beam kinetic energy any existing polarized target may be always considered to be very thin for $\Delta\sigma_L(np)$ experiment and we can replace the exponential functions in (3.3) by linear ones. We obtain :

$$-\Delta\sigma_L(P_T^+) = \frac{1}{|P_B\ P_T^+|\ n_H\ d} \times \left(1 - \frac{N(++)}{N(-+)}\right), \qquad (3.5a)$$
$$-\Delta\sigma_L(P_T^-) = \frac{1}{|P_B\ P_T^-|\ n_H\ d} \times \left(1 - \frac{N(--)}{N_(+-)}\right). \qquad (3.5b)$$

At any JINR accelerator energy this approximation provides an error smaller that 6×10^{-7} and can never be recognized.

However, there are small contributions from ^{13}C and ^3He, which may be slightly polarized. This contribution was estimated to be $\pm$ 0.3 % in [1,2].

For $\Delta\sigma_L$, without a lost of generality, we will consider only one $|P_T| = P_T^+$ sign and we denote the effect, measured with a completely filled target in ((3.3a) as

$$\exp(-E) = \exp(-\frac{1}{2}\Delta\sigma_L\ |P_B\ P_T|\ n_H\ d\ ). \qquad (3.6)$$

Using (2.4a), (2.4b) and the horizontal mode of the incomplete target filling, we obtain

$$\frac{NH(++)}{NH(-+)} = \frac{a \times \exp\ (-F) \times \exp\ (-E) + (1-a)}{a \times \exp\ (-F) \times \exp(+E) + (1-a)}. \qquad (3.7)$$

Below we will considered F from (3.1) as the unpolarized background from all target atoms. We put $\exp(\pm\ E) = 1 \pm\ E$, and rewrite (3.7) :

$$\frac{NH(++)}{NH(-+)} = \frac{1 - \dfrac{E\ a\ \exp(-F)}{a\ \exp(-F) + (1-a)}}{1 + \dfrac{E\ a\ \exp(-F)}{a\ \exp(-F) + (1-a)}} \qquad (3.8)$$

We applied the binomial development $(1-x)/(1+x) \simeq (1-2x)$ for small x. In our case the error is smaller than 2×10^{-6}. Using this, we obtain the relation for $-\Delta\sigma_L$, similar to (3.5) :

$$-\Delta\sigma_L = \frac{1}{|P_B\ P_T|\ n_H\ d\ C_{corr}} \times \left(1 - \frac{NH(++)}{NH(-+)}\right). \qquad (3.9)$$

The multiplicative correction factor

$$C_{corr} = \frac{a\ \exp(-F)}{a\ \exp(-F) + (1-a)}, \qquad (3.10)$$

depends on a and on the background, but is independent on the measured $\Delta\sigma_L$ value. It holds $C_{corr} \leq a$ where the equality is valid for $\exp(-F) = 1$, i.e no background. The equality also occurs, if the same amount of the target material is condensed in a shorter target (vertical filling mode) of the length $d \times a$.

4 Experimental set-up

The $\Delta\sigma_L(np)$ experimental set-up was described in [1,2]. We mention here only essential items, which are important for the data analysis and results, as well as modifications and improvements of the apparatus and of the experimental conditions.

Figure 1 shows both polarized deuteron and polarized free neutron beam lines [5,6], the two polarimeters [30,31], the neutron production target (BT), the collimators, the spin rotation magnet (SRM), PPT [3,4,32], the neutron monitors M1, M2, transmission detectors T1, T2, T3 and the neutron beam profile monitor NP. The associated electronics was described in [1,2] and the data acquisition system in [7].

Accelerated deuterons were extracted at energies 3.20, 3.60 and 4.40 GeV for the $\Delta\sigma_L(np)$ measurements as well as at 1.60 GeV for the polarimetry purposes. Their beam momenta p_d were known with the relative accuracy of $\sim \pm 1$ %. The intensity of primary polarized deuteron beam was increased by a factor $\sim$ 3 to 4 with respect to the 1995 run. The average deuteron intensity over the run was $2.12\times10^9 d$/cycle. It was continuously monitored using two calibrated ionization chambers placed in the focal points F3 and F4 of the deuteron beam line.

The beam of free quasi-monochromatic neutrons, polarized along the vertical direction, was obtained by break-up at 0° of vector polarized deuterons in BT. Neglecting the BT thickness, neutrons have a laboratory momentum $p_n = p_d/2$ with a momentum spread of FWHM $\simeq$ 5 % [33]. BT contained 20 cm Be with the cross section of 8×8 cm^2. The passage of deuterons through air, windows and the BT matter provided a decrease of the deuteron beam energy by 20 MeV in the BT center and the mean neutron energy decreased by 10 MeV [1,2]. For the results the energies and laboratory momenta in the BT center are quoted, for the beam polarization measurements the extracted beam energies were used.

The values and directions of the neutron and proton beam polarizations after break-up, $\vec{P}_B(n)$ and $\vec{P}_B(p)$, respectively, are the same as the vector polarization $\vec{P}_B(d)$ of the incident deuteron beam [34,35].

The measurement of $P_B(d)$ was carried out by the four-arm *dp* beam line polarimeter [30]. Deuterons, scattered on the liquid hydrogen target, were analyzed by a magnetic field. The *dp* polarimeter may use a high intensity of deuterons. It accurately determined the elastic *pd* scattering asymmetry at $T_{kin}(d) = 1.60$ GeV, where the analyzing power of this reaction is well known, and at the four-momentum transfer square t = –0.015 (GeV/c)^2 ($\theta_{lab}(d) \sim 7.7°$), close to the maximal analyzing power value [36]. In principle, the $P_B(d)$ needs to be determined at one energy only, since no depolarizing resonance exists [30]. On the other hand, the measurement requires to change the deuteron energy and to extract deuterons in another beam line, which is a time-consuming operation. This polarimeter was used only once before the data acquisition and gives an average for positive and negative signs of the vector polarization $|P_B(d)| = 0.524 \pm 0.010$. A possible absolute systematic error of this measurement is $\pm$0.010.

Another four-arm beam polarimeter [31] with small acceptance of 7.1×10^{-4} sr continuously monitored $P_B(p)$ value during the data acquisition. The deuteron beam, considered as a beam of quasifree protons and neutrons, was scattered on CH_2 target at 14° lab. This polarimeter measured the *pp* left-right asymmetry on hydrogen and carbon at $T_{kin}(p) = T_{kin}(d)/2$. At $T_{kin}(p) = 0.800$ GeV, the simultaneous measurement together with the *dp* polarimeter gave the asymmetry $\epsilon(CH_2) = 0.2572 \pm 0.0071$. A subtraction of the carbon and inelastic contributions provided the *pp* asymmetry on hydrogen $\epsilon(pp) = 0.2661 \pm 0.0073$.

The *pp* analyzing power A_{oono} was taken from the energy fixed GW/VPI-PSA [24] (SP99, solution 0.800 GeV) as well as from SG-PSA [29] (solution 0.795 GeV). The $A_{oono}(pp)$ predictions at 0.800 GeV were:

GW/VPI-PSA ... 0.4871 ± 0.0034,
SG-PSA ... 0.4821 ± 0.0009.

The mean value $A_{oono}(pp) = 0.4846 \pm 0.0017$ and the measured asymmetry provided $P_B(p)| = |P_B(d)| = 0.549 \pm 0.015$.

The weighted average of both independent results from the two polarimeters gives

$$|P_B(p)| = 0.532 \pm 0.008,$$

used for the calculations of the present $\Delta\sigma_L$ data. This is in excellent agreement with the value $|P_B(n)| = |P_B(d)| = 0.533 \pm 0.009$ measured in 1995 with the *dp* polarimeter at $T_{kin}(d) = 1.662$ GeV and used in [1,2].

Also in 1995, at 0.831 GeV, the *pp* polarimeter provided $\epsilon(CH_2) = 0.246 \pm 0.016$ only. If we apply the present ratio of $\epsilon(pp)/\epsilon(CH_2) = 1.0346$, neglecting the small energy difference, we have $\epsilon(pp) = 0.255 \pm 0.017$. The discrete energy $A_{oono}(pp)$ predictions from GW/VPI-PSA [24] (SP99, solution 0.850 GeV) and from SG-PSA [29] (solution 0.834 GeV) give the mean value of 0.4824 ± 0.0048. We obtain $P_B(p)| = |P_B(d)| = 0.528 \pm 0.035$, in agreement with the former *dp* polarimeter value.

Note that we have used the discrete energy PSA for the *pp* analyzing power calculations. Both PSA are locally energy dependent and describe the measured observables at its own energies. The energy dependent PSA is not an adequate tool for the polarimetry purposes, since the A_{oono} fit at a given energy may be smeered by all other observables fitted in a wide energy range.

We observed that $|P_b(d)|$ decreased during the running time *tm* (hours) as

$$P_d(tm) = P_d(tm = 0)\ (1 - 0.00154 \cdot tm)\ . \qquad (4.1)$$

The error of the linear term is $\pm$ 0.00013. This decrease, due to an unknown effect in the ion source was independent on the beam energy and was taken into account for the present results. The global relative systematic error of $|P_b(d)|$ from all sources was $\pm$1.7 %.

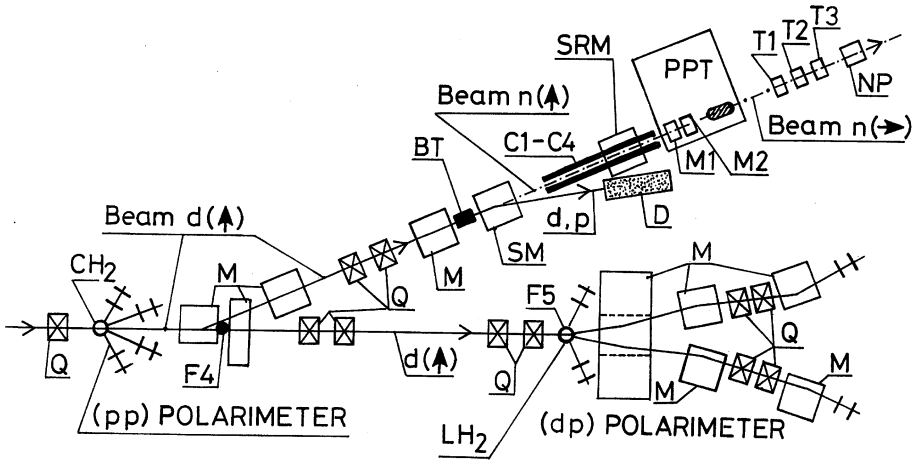

Fig. 1. Layout of the beam lines in the experimental hall (not in the scale). The meaning of the symbols: full lines ... vector polarized deuteron beams with $\vec{P}_B(d)$ oriented along the vertical direction $d(\uparrow)$, dash-dotted line ... polarized neutron beam, $n(\uparrow)$ ... neutrons polarized vertically, $n(\rightarrow)$ ... neutrons polarized longitudinally, BT ... neutron production target, D ... beam-dump for charged particles, SM ... sweeping magnet, SRM ... spin rotating magnet M ... dipole magnets, Q ... quadrupoles, C1 to C4 ... neutron beam collimators, M1, M2, T1, T2, T3, neutron detectors, PPT ... polarized proton target, NP ... neutron beam profile monitor, LH_2 ... liquid hydrogen target of the *dp* polarimeter, CH_2 ... target of the *pp* polarimeter, F4, F5 ... focal points

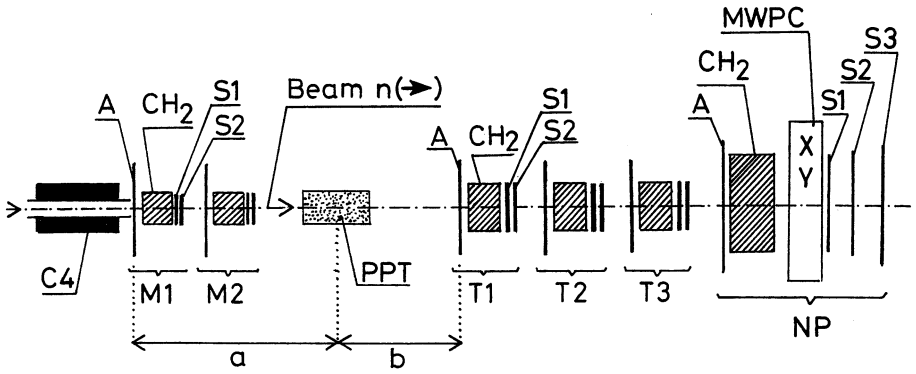

Fig. 2. Experimental set-up for the $\Delta\sigma_L(np)$ measurement (not in the scale). The meaning of the symbols: C4 ... last neutron beam collimator, 25 mm in diameter, M1, M2 ... monitor neutron detectors, T1, T2, T3 ... transmission neutron detectors, NP ... neutron beam profile monitor, CH_2 ... radiators (dimensions in text), A ... anticoincidence scintillation counters, S1, S2, S3 concidence scintillation counters, MWPC ... two multi-wire proportional chambers, distance a = 235 cm, distance b = 655 cm

The dimensions and positions of the iron and brass collimators C1-C4 (Fig. 1) were as described in [1,2]. The accurate measurement of the collimated neutron beam profiles were performed in a dedicated run, using nuclear emulsions. During the data acquisition, the position and the X,Y-profiles of the neutron beam were continuously monitored by the neutron beam profile monitor (NP), placed close downstream from the last transmission detector.

In order to rotate the neutron beam polarization from the vertical to the longitudinal direction, a spin-rotating magnet (SRM) was used. The SRM field map was carefully measured and the magnetic field was continuously monitored by a Hall probe. The uncertainty of the magnetic field integral within the neutron beam path area may provide a small additional systematic error of ± 0.2 %.

The frozen-spin polarized proton target, reconstructed to the movable device [3,4,8,32] was used. The target material was 1,2-propanediol ($C_3H_8O_2$) with a paramagnetic Cr^V impurity having the spin concentration of 1.5×10^{20} cm^{-3} [37]. The propanediol beads were loaded in a thin-wall teflon container 200 mm long and 30 mm in diameter, placed inside the dilution refrigerator.

The weight of the propanediol beads for the completely filled container is W = 94.88 g and the total number of polarizable hydrogen atoms on the beam neutron path gives $n_H \times d = 8.878\ 10^{23}$ cm^{-2}. In the present experiment the measured weight of the beads was W' = (73.25 $+0.80, -0.20$) g. The ratio of the weights is a = W'/W = 0.772. For our $\Delta\sigma_L$ calculation we have considered the horizontal filling mode of (3.9). The correction factor C_{corr} is a function of a and weakly depends on the background, as defined in (3.10). The background transmission ratio for the completely filled target was measured in [1,2] and gave $\exp(-F) = 0.779$. Using those values we obtain $C_{corr} = 0.725$ and $n_H\ d\ C_{corr} = (6.44 \pm 0.19)\ 10^{23}$ cm^{-2}. Since in our energy region the spin-averaged total cross sections are fairly constant, we have neglected a possible dependence of C_{corr} on energy. The relative systematic error of ± 1.5 % covers this uncertainty and was included in the final error in quadrature. The $\Delta\sigma_L$ results were calculated using (3.9) with the transmission ratios measured separately for P_T^+ and P_T^-.

We note that for a shorter target of the beam diameter size $C_{corr} = a$ and $n_H \times d \times a = 6.854\ 10^{23}$ cm^2. The difference of these two filling modes is 6.4 %.

The P_T measurements were carried out using a computer-controlled NMR system. The values of negative proton polarization were –0.772 at the beginning of data taking and –0.701 at the end (after 64 hours). The positive

Table 1. Total statistics of recorded events after the first step of the data analysis as functions of energy and the P_B and P_T signs. The count numbers for the monitors M1, M2 and the transmission detectors T1, T2 and T3 are given in 10^6 units. Here 2 ΣT/3 ΣM is calculated from the global statistics of the three transmission detectors and of the two monitors. The energy of neutrons produced in the BT center is given

T_{kin}	Sign		Statistics of detectors					$2\Sigma T/3\Sigma M$
(GeV)	P_B	P_T	M1	M2	T1	T2	T3	
1.59	+	+	4.9985	4.9483	4.3994	4.2241	3.9690	0.84399
1.59	−	+	5.0030	4.9460	4.4048	4.2299	3.9715	0.84472
1.79	+	+	7.8152	7.6557	6.7115	6.4426	6.0965	0.83213
1.79	−	+	7.8170	7.6798	6.7151	6.4392	6.0976	0.82928
1.79	+	−	12.2593	12.0137	10.3517	10.0732	9.4718	0.82112
1.79	−	−	12.2687	12.0306	10.3570	10.0837	9.4827	0.82097
2.20	+	+	15.9493	15.4885	13.3503	12.3471	12.1170	0.80188
2.20	−	+	16.0665	15.6043	13.4595	12.4498	12.2066	0.80234
2.20	+	−	17.9478	17.4144	14.7624	14.1608	13.6531	0.80267
2.20	−	−	17.8615	17.3222	14.6809	14.0962	13.5831	0.80265

P_T values were 0.728 and 0.710 after 34 hours, respectively. This corresponds to the relaxation times of 1358 hours for P_T^+ and 663 hours for P_T^-. The relative uncertainty of the measured P_T values has been estimated to be ±5 %. This error includes the uniformity meaurements using the NMR data from the three coils.

The configuration of the two neutron intensity monitors M1 and M2 and the three transmission detectors T1, T2 and T3 is shown in Fig. 2. The detectors were of similar design and the electronics were identical [1,2]. Each detector consisted of a CH_2 converter, 60 mm thick, placed behind a large veto scintillation counter A. Charged particles emitted forward were detected by two counters S1 and S2 in coincidence. The monitor converters and S1, S2 counters were 30 mm in diameter and the corresponding elements of the transmission detectors were 90, 92 and 96 mm for T1, T2 and T3, respectively. The NP array, also shown in Fig. 2, was similar as the neutron detectors. The two multiwire proportional chambers behind the converter were protected by its veto A and triggered by S1, S2 and S3 counters in coincidence.

The result of $\Delta\sigma_L$ is independent on the neutron beam intensity, if a probability of quasi-simultaneous detection of two neutrons in one transmission detector may be neglected. The efficiency of detector are then limited and each of the detectors is independent of any other one [1].

Dedicated tests were performed during an additional run with a high intensity unpolarized deuteron beam. Using the same transmission set-up the neutron carbon total cross section $\sigma_{tot}(n-C)$ was determined at $T_{kin}(n) = 1.5$ GeV. For this purpose a number of carbon targets with different thicknesses were inserted in the neutron beam line instead of the PPT. The measured $\sigma_{tot}(n-C)$ value agrees with the data from the compilation "Cross Sections of Particles and Nuclei with Nuclei" [38].

5 Data analysis

For each accelerator cycle the following main information was recorded and displayed by the data acquisition system:

- rates of the two calibrated ionization chambers used as the primary deuteron beam intensity monitors,
- rates of coincidences and accidental coincidences for the two neutron detectors M1 and M2 used as the intensity monitors of the neutron beam incident on the PPT,
- rates of coincidences and accidental coincidences for the three neutron transmission detectors T1, T2 and T3,
- rates of the left and right arms of the *pp* beam polarimeter.

At the beginning of the run, statistics at 2.20 and 1.79 GeV with P_T^- were recorded. Then the data were taken at 2.20, 1.79 GeV and 1.59 GeV with P_T^+. At the latter energy, the data with P_T^- could not be measured.

The recorded data were then analyzed in two steps. In the first step, "bad" files were removed, as well as "empty" cycles and cycles with incorrect labels of P_B signs. The number of "bad" cycles for the cumulated statistics represented a few tenth of percent. Remaining event statistics over the run for different detectors are shown in Table 1, separately for each combination of the $\vec{P}_B$ and $\vec{P}_T$ direction. With decreasing energy σ_{0tot} for all target elements decreases and the global target transmission ratio $\Sigma T/\Sigma M$ increases, as expected. Since the statistics listed in one row were taken simultaneously, we see also a monotonous decrease as a function of the detector distance from the target.

The second step of the data analysis used the previously selected events in order to check the stability of neutron detectors, to determine parameters of the statistical distribution and to obtain the final results. The

Table 2. The measured $-\Delta\sigma_L(np)$ values at different energies for the two opposite target polarizations, for the individual transmission detectors and for the cumulated statistics. The instrumental asymmetry (IA) and the averaged $-\Delta\sigma_L(np)$ data were deduced. The quoted errors are statistical only

T_{kin} (GeV)	Transm. detectors	$-\Delta\sigma_L(P_T^+)$ (mb)	$-\Delta\sigma_L(P_T^-)$ (mb)	IA (mb)	Average $-\Delta\sigma_L$ (mb)
1.59	T1	$+4.7 \pm 3.9$			$+4.7 \pm 3.9$
	T2	$+5.5 \pm 3.9$			$+5.5 \pm 3.9$
	T3	$+2.0 \pm 4.0$			$+2.0 \pm 4.0$
	T1,2,3	$+4.1 \pm 2.9$			$+4.1 \pm 2.9$
1.79	T1	$+0.7 \pm 3.0$	$+2.5 \pm 2.3$	-0.9 ± 1.9	$+1.6 \pm 1.9$
	T2	-4.2 ± 3.1	$+0.2 \pm 2.3$	-2.2 ± 1.9	-2.0 ± 1.9
	T3	-0.9 ± 3.1	-0.3 ± 2.4	-0.3 ± 2.0	-0.6 ± 2.0
	T1,2,3	-1.5 ± 2.2	$+0.9 \pm 1.7$	-1.2 ± 1.4	-0.3 ± 1.4
2.20	T1	$+3.4 \pm 2.1$	$+2.0 \pm 1.8$	$+0.7 \pm 1.4$	$+2.7 \pm 1.4$
	T2	$+4.1 \pm 2.1$	-2.0 ± 1.9	$+3.0 \pm 1.4$	$+1.0 \pm 1.4$
	T3	-0.1 ± 2.1	$+0.4 \pm 1.9$	-0.2 ± 1.4	$+0.1 \pm 1.4$
	T1,2,3	$+2.5 \pm 1.5$	$+0.1 \pm 1.3$	$+1.3 \pm 1.0$	$+1.3 \pm 1.0$

transmission ratios as functions of time were analyzed for each combination of the individual M and T detectors, at any neutron energy and the P_T sign. No significant time dependence of checked values was observed. The results were extracted using the relations (2.5a), (2.5b) and (3.9). Each of them contains a hidden contribution [13] from the instrumental asymmetry (IA) due to the counter misalignments and to the residual perpendicular components in the beam polarization. For this reason a half-sum of (2.7), i.e. a simple average, provides $\Delta\sigma_L$, whereas a half-difference gives the IA value, as has been discussed in [13].

The IA contribution could be hardly suppressed. Due to the longitudinal $\vec{P}_B$ direction and the full kinematic axial symmetry, it is usually small for the $\Delta\sigma_L$ experiment. It may be very large for the $\Delta\sigma_T$ measurement, where no symmetry exists. The results strongly depend on the detector stabilities and their fixed positions over the data acquisition with the both P_T signs. For stable detectors, $\Delta\sigma_L$ is expected to be found time independent and equal for each transmission detector, within statistical errors. In contrast, the IA value depends on each individual neutron detector, including the monitors.

In Table 2 are listed the $-\Delta\sigma_L(np)$ values for both signs of P_T, their half differences and the half-sums. All results were obtained using common statistics from both monitors M1 and M2. The abreviation T1,2,3 signify that the entire statistics from all detectors were taken into account.

It can be seen that IA was considerably smaller for the detectors T1 and T3 than for T2. The IA values change its sign for almost all detectors between 1.79 and 2.20 GeV. Since the elements of the detectors were not moved during the run, we assume that the residual perpendicular components in $\vec{P}_B$ were oposite. The relative normalization and systematic errors, from different sources are summarized as follows:

- Beam polarization including time dependence $\pm$ 1.7 %
- Target polarization ..... $\pm$ 5.0 %
- Number of the polarizable hydrogen atoms including filling mode ..... $\pm$ 1.5 %
- Magnetic field integral of the neutron spin rotator ..... $\pm$ 0.2 %
- Polarization of other atoms ..... $\pm$ 0.3 %
- Inefficiencies of veto counters ..... $\pm$ 0.1 %

- Total of the relative systematic errors ..... $\pm$ 5.5 %
- Absolute error due to the extrapolation of results towards 0° ..... < 0.04 mb

6 Results and discussion

The final $-\Delta\sigma_L(np)$ values are presented in Table 3 and shown in Fig. 3. The statistical and systematic errors are quoted. The total errors are the quadratic sums of both uncertainties. Since the measurement at 1.59 GeV was carried out with one P_T sign only, the instrumental ϕ-asymmetry could not be removed using (7). At this energy, we have added the weighted average of the absolute IA values at 1.79 and 2.20 GeV ($\pm$ 1.18 mb) in quadrature to the systematic error.

The results from [1,2] together with the existing $\Delta\sigma_L(np)$ data [13-18], obtained with free polarized neutrons at lower energies, are also shown in Fig. 3. We added the point at 19.7 MeV recently measured at TUNL [22] in order to show the $\Delta\sigma_L(np)$ energy dependence in a large energy range. The new results smoothly connect with the data at lower and at higher energies and suggest even faster decrease above 1.1 GeV than previously

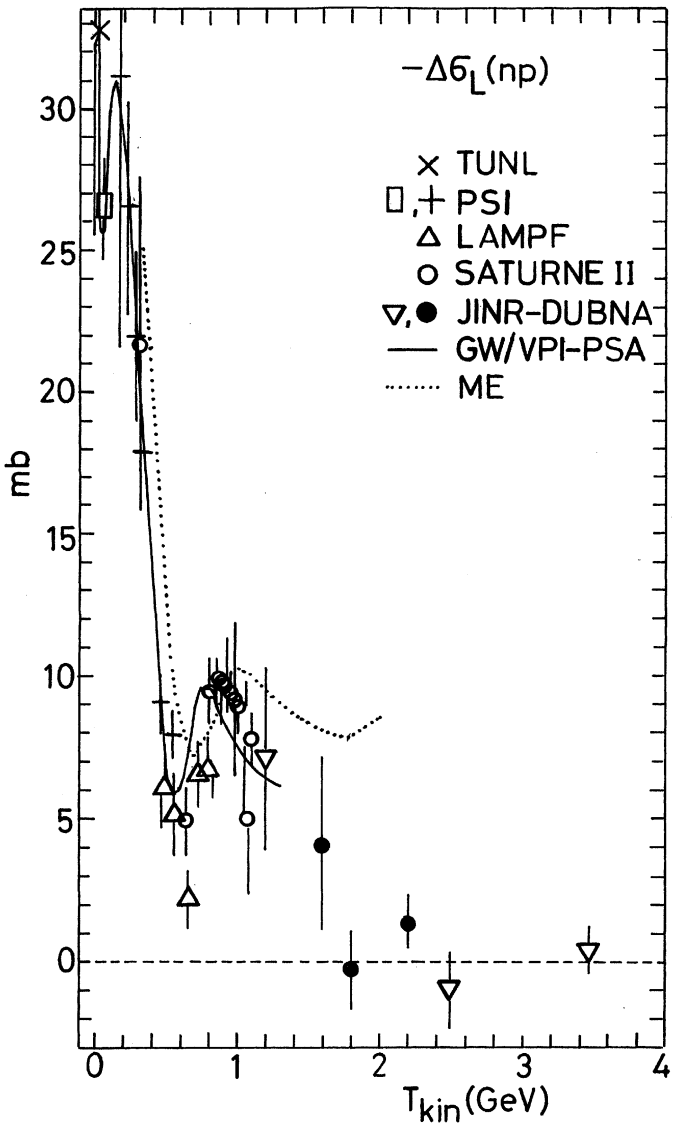

Fig. 3. Energy dependence of $-\Delta\sigma_L(np)$. The meaning of the symbols: • ... this experiment, ▽ ... JINR [1,2], × ... TUNL [22], rectangle ... PSI [18], + ... PSI [16], △ ... LAMPF [17], ○ ... SATURNE II [13,14], full curve ... GW/VPI-PSA [24] (SP99 solution), dotted curve ... meson-exchange model [41]

observed [1,2]. The solid curve represent the energy dependent GW/VPI-PSA [24] (SP99 solution) fit of this observable over the interval from 0.02 to 1.3 GeV. Above 0.8 GeV the fit considerably differs from that presented in [1,2]. This is due to a large amount of *np* and *pp* data points for different observables, included into the GW/VPI-PSA database. The database also contains the previous JINR $\Delta\sigma_L(np)$ result at 1.19 GeV. Unfortunately, the number of $\Delta\sigma_L(np)$ points is too small with respect to a prevalence of all other scattering data. Consequently the energy dependent GW/VPI-PSA fit is only in a qualitative agreement with the measured values. Above 1.1 GeV (SATURNE II) the *np* database is insufficient at all. Nevertheless, the high energy part of the PSA fit follows fairly well the behaviour of the experimental data.

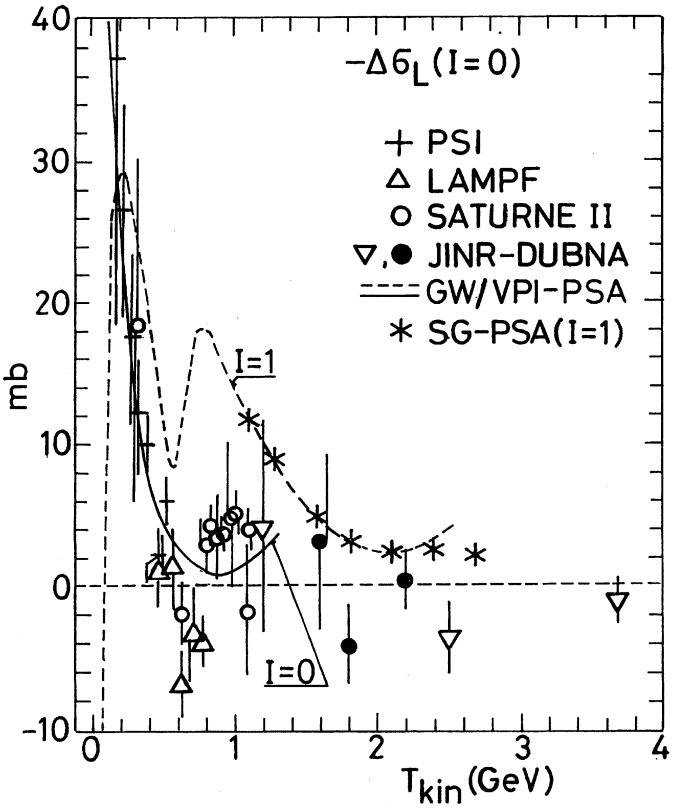

Fig. 4. Energy dependence of the $-\Delta\sigma_L(I=0)$ calculated from measured *np* data and the known *pp* values. The *np* data at the same energies as in Fig. 3 are used and the $I=0$ results are denoted by the same symbols. The full line is calculated from the common *np* and *pp* GW/VPI-PSA [24] (SP99 solution). The dashed line is the $-\Delta\sigma_L(I=1)$ prediction from the same GW/VPI-PSA, and ($\star$) are $I=1$ predictions from SG-PSA [29]

Using (2.11), one can deduce $\Delta\sigma_L(I=0)$ values from the obtained $\Delta\sigma_L(np)$ results and the existing $\Delta\sigma_L(pp)$ data. For this purpose, we used the ANL-ZGS [39] and SATURNE II [40] $\Delta\sigma_L(pp)$ data. The results are given in Table 4 and plotted in Fig. 4. Since the *pp* data are accurate, the $-\Delta\sigma_L(I=0)$ values have roughly two times larger errors than the *np* results. For this reason, an improved accuracy of *np* measurements is important.

In Fig. 4 are also plotted the $-\Delta\sigma_L(I=0)$ values from [1,2] together with those using the $\Delta\sigma_L(np)$ data sets [13-17]. All results are compatible and suggest a plateau or a maximum around 1.5 GeV, followed by a rapid decrease with increasing energy. The solid curve was calculated from the *np* and *pp* GW/VPI-PSA fits. An apparent disagreement with the measured data points above 0.6 GeV is related to a fairly rough PSA description of *np* data. The difference between the GW/VPI-PSA fit and the data, shown in Fig. 3, increases twice for the $I=0$ energy dependence in Fig. 4.

In the same figure are plotted the $-\Delta\sigma_L(I=1)$ PSA fits for a comparison. The GW/VPI-PSA for *pp* elastic scattering cover the energy range up to 2.55 GeV (dashed line) and SG-PSA up to 2.7 GeV (stars above 1.1 GeV).

Table 3. The final $-\Delta\sigma_L(np)$ results. Total errors are quadratic sums of the statistical and systematic ones. The energy and the laboratory momenta of the neutron beam in the production target center are given

T_{kin} (GeV)	p_{lab} (GeV/c)	$-\Delta\sigma_L(np)$ (mb)	Statis. error (mb)	System. error (mb)	Total error (mb)
1.59	2.35	+4.1	±2.9	±1.20	±3.1
1.79	2.56	−0.3	±1.4	±0.02	±1.4
2.20	2.99	+1.3	±1.0	±0.07	±1.0

Table 4. The $-\Delta\sigma_L(I=0)$ values deduced from the present $\Delta\sigma_L(np)$ results and existing $\Delta\sigma_L(pp)$ data. The energies of $\Delta\sigma_L(pp)$ data and corresponding references are also listed

$T_{kin}(np)$ (GeV)	$T_{kin}(pp)$ (GeV)	$-\Delta\sigma_L(pp)$ (mb)	Ref. pp	$-\Delta\sigma_L(I=0)$ (mb)
1.59	1.594	$+4.93 \pm 0.30$	[40]	$+3.2 \pm 6.2$
1.79	1.798	$+3.39 \pm 0.10$	[40]	-4.0 ± 2.8
2.20	2.176	$+2.28 \pm 0.10$	[39]	$+0.3 \pm 2.0$

Both PSA contain almost all existing data and their predictions at low energies are in excellent agreement.

Some dynamic models predicted the $\Delta\sigma_{L,T}$ behaviour for np and pp transmissions. Below 2.0 GeV, an usual meson exchange theory of NN scattering [41] gives the $\Delta\sigma_L(np)$ energy dependence as shown by the dotted curve in Fig. 3. It can be seen that this model provides only a qualitative description at low energies and disagree considerably with the data above 1 GeV.

In [1,2] was discussed a model of a nonperturbative flavour-dependent interaction between quarks, induced by a strong fluctuation of vacuum gluon fields, i.e. instantons. An energy dependent contribution to $\Delta\sigma_L(np)$ was qualitatively estimated. Concerning this model we refer to [1,2] and to references therein, since no new relevant predictions are available.

The investigated energy region corresponds to a possible generation of heavy dibaryons with masses $M > 2.4$ GeV (see review [42]). For example, a model [43,44] predicts the formation of a heavy dibaryon state with a color octet-octet structure.

The possible manifestation of exotic dibaryons in the energy dependence of different pp and np observables was predicted by another model [45-49]. The authors used the Cloudy Bag Model and an R-matrix connection to long-range meson-exchange force region with the short-range region of asymptotically free quarks. The model gives the lowest lying exotic six-quark configurations in the isosinglet and the spin-triplet state $^3S_1$ with the mass M = 2.63 GeV ($T_{kin} = 1.81$ GeV). For the $I = 0$ state, the $^3S_1$ partial wave is expected to be predominant. The measurement of $\Delta\sigma_T$ observable for np transmission and its determination for $I = 0$ may provide a significant check. Since $\Delta\sigma_T$ for arbitrary isospin state contains no uncoupled spin-triplet state, a possible dibaryon resonance effect in $^3S_1$ may be less diluted. Moreover, in the difference of both quantities the spin-singlet contributions vanish.

The three optical theorems determine the imaginary parts of the nonvanishing forward amplitudes as shown in (2.8) to (2.10). A maximum in $I = 0$ amplitudes or in their combinations dominated by the spin-triplet states will be a necessary condition for the predicted resonance. The sufficient condition may be provided by real parts. For np scattering they can be determined by measurements of observables in the experimentally accessible backward direction, as was shown in [50].

The $I = 0$ spin dependent total cross sections represent a considerable advantage for studies of possible resonances. This is in contrast with the $I = 1$ system where the lowest lying exotic six-quark configuration corresponds to the spin-singlet state $^1S_0$. This state is not dominant and is hard to be separated it in the forward direction. Scattering data directly related with the spin-singlet amplitude at other angles are preferable to be measured.

7 Conclusions

The new results are presented for the transmission measurements of the $\Delta\sigma_L(np)$ energy dependence in the Dubna Synchrophasotron energy region below 3.7 GeV. Measured $\Delta\sigma_L(np)$ values are compatible with the existing np results, using free neutrons. The rapid decrease of $-\Delta\sigma_L(np)$ values from 1.1 to 2.0 GeV is confirmed. It is found to be faster than expected from the previous measurement.

The $\Delta\sigma_L(I = 0)$ quantities, deduced from the measured $\Delta\sigma_L(np)$ values and the existing $\Delta\sigma_L(pp)$ data, are also presented. They indicate a plateau or a maximum around 1.5 GeV, followed by a rapid decrease with energy.

Obtained results are compared with the dynamic model predictions and with the recent GW/VPI-PSA fit. A necessity of further $\Delta\sigma_L(np)$ measurements and new $\Delta\sigma_T(np)$ data in the kinetic energy region above 1.1 GeV is emphasized.

Acknowledgements. Authors thank the JINR LHE and LNP directorates for support of these investigations. Discussions with V.N.Penev and B.Peyaud solved several problems. We are grateful to J.Ball, M.P.Rekalo and I.I.Strakovsky for helpful suggestions.

The measurements were possible due to the JINR directorate Grant. The work was supported in part by the International Science Foundation and Russian Government through Grant No. JHW 100, by the International Association for the Promotion of Cooperation with Scientists from the Independent States of the Former Soviet Union (INTAS) through Grant No. 93-3315, by the Russian Foundation for Basic Research through Grants RFBR-93-02-03961, RFBR-93-02-16715, RFBR-95-02-05807, RFBR-96-02-18736 and by the Fundamental Nuclear Physics Foundation Grant 122.03.

References

1. B.P. Adiasevich, et al., Zeitschrift für Physik C **71**, 65 (1996)
2. V.I. Sharov, et al., JINR Rapid Communications **3[77]-96**, 13 (1996)
3. F. Lehar, et al., Nucl.Instrum.Methods A **356**, 58 (1995)
4. N.A. Bazhanov, et al., Nucl.Instrum.Methods A A **372**, 349 (1996)
5. I.B. Issinsky, et al., Acta Physica Polonica B **25**, 673 (1994)
6. A. Kirillov, et al., "Relativistic Polarized Neutrons at the Laboratory of High Energy Physics, JINR", Preprint JINR E13-96-210, Dubna, 1996
7. E.V.Chernykh, S.A.Zaporozhets, Proceedings of the ES-ONE International Conference "RTD 94", Editors R.Pose, P.U. ten Kate, E.W.A.Lingeman, Preprint E10,11-95387, JINR, Dubna 1995, p.179
8. N.G. Anischenko, et al., JINR Rapid Communications **N6[92]-98**, 49 (1998)
9. D.P. Grosnick, et al., Phys.Rev. D **55**, 1159 (1997)
10. C.Lechanoine-Leluc, F.Lehar, Rev.Mod.Phys. **65**, 47 (1993)
11. I.P.Auer, et al., Phys.Rev.Lett. **46**, 1177 (1981)
12. W.Grein, P. Kroll, Nucl. Phys. A **377**, 505 (1982)
13. F.Lehar, et al., Phys.Lett. **189B**, 241 (1987)
14. J.-M. Fontaine, et al., Nucl.Phys. B **358**, 297 (1991)
15. J.Ball, et al., Zeitschrift für Physik C **61**, 53 (1994)
16. R.Binz, et al., Nucl.Phys. A **533**, 601 (1991)
17. M. Beddo, et al., Phys.Lett. **258B**, 24 (1991)
18. P.Haffter, et al., Nucl.Phys. A **548**, 29 (1992)
19. J. Brož, et al., Zeitschrift für Physik A **359**, 23 (1997)
20. W.S.Wilburn, et al., Phys.Rev. C **52**, 2352 (1995)
21. J.Brož, et al., Zeitschrift für Physik A **354**, 401 (1996)
22. J.R.Walston, PhD Thesis, North Carolina State University, 1998 (unpublished)
23. B.W.Raichle, PhD Thesis, North Carolina State University, 1997 (unpublished)
24. R.A.Arndt, et al., Phys.Rev. C **56**, 3005 (1997)
25. J.Bystrický, F.Lehar, P.Winternitz, J.Physique (Paris) **39**, 1 (1978)
26. S.M.Bilenky, R.M.Ryndin, Phys.Lett. **6**, 217 (1963)
27. R.J.N.Phillips, Nucl.Phys. **43**, 413 (1963)
28. J. Ball, et al., Nuovo Cimento A **111**, 13 (1998)
29. J.Bystrický, C.Lechanoine-LeLuc, F.Lehar, Eur.Phys.J. C **4**, 607 (1998)
30. V.G. Ableev, et al., Nucl.Instrum.Methods A **306**, 73 (1991)
31. L.S.Azhgirey, et al., Pribory i Tekhnika Experimenta **1**, 51 (1997), transl. Instrum. and Exp.Techniques **40**, 43 (1997)
32. N.A. Bazhanov, et al., Nucl.Instrum.Methods A **402**, 484 (1998)
33. V.G.Ableev, et al., Nucl. Phys. A **393**, 941 (1983) and A **411** 541E (1983)
34. E.Cheung, et al., Phys.Lett. B **284**, 210 (1992)
35. A.A. Nomofilov, et al., Phys.Lett. B **325**, 327 (1994)
36. V.Ghazikhanian, et al., Phys.Rev. C **43**, 1532 (1991)
37. E.I.Bunyatova, R.M.Galimov, S.A.Luchkina, "Investigation of Stable Paramagnetic HMBA Complex in Different Solvents", Preprint JINR 12-82-732, Dubna 1982
38. V.S.Barashenkov, "Secheniya Vzaimodeistviya Chastits i Yader s Yadrami." JINR Publishing Department, Dubna, 1993
39. I.P.Auer, et al., Phys.Rev.Lett. **41**, 354 (1978)
40. J.Bystrický, et al., Phys.Lett. **142B**, 141 (1984)
41. T.-S.H.Lee, Phys.Rev. C **29**, 195 (1984)
42. I.I.Strakovsky, Fiz. Elem. Chastits At. Yadra **22**, 615 (1991), transl. Sov.J.Part.Nucl. **22**, 296 (1991)
43. B.Z.Kopeliovich, F.Niedermayer, Zh.Eksp.Teor.Fiz. **87**, 1121 (1984), transl. Sov.Phys. JETP **60**(4), 640 (1984)
44. B.Z.Kopeliovich, Fiz. Elem. Chastits At. Yadra **21**, 117 (1990), transl. Sov.J.Part.Nucl. **21**(1), 49 (1990)
45. P.LaFrance, E.L.Lomon, Phys.Rev. D **34**, 1341 (1986)
46. P.Gonzales, P.LaFrance, E.L.Lomon, Phys.Rev. D **35**, 2142 (1987)
47. P.LaFrance, Can.J.Phys. **68**, 1194 (1990)
48. E.L. Lomon, Colloque de Physique (France) **51**, C6-363 (1990)
49. P. LaFrance, E.L. Lomon, Proceedings of the International Conference "Mesons and Nuclei at Intermediate Energies", Dubna, 3-7 May 1994, Editors: M.Kh. Khankhasaev, Zh.B. Kurmanov, World Scientific, Singapore, 1995-XV, p.97
50. J. Ball, et al., Eur.Phys.J. C **5**, 57 (1998)